CHIN. PHYS. LETT. Vol. 37, No. 6 (2020) 062801

Stabilization of Short Wavelength Resistive Ballooning Modes by Ion-to-Electron Temperature and Gradient Ratios in Tokamak Edge Plasmas *

Jian-Qiang Xu(许健强)**, Xiao-Dong Peng(彭晓东), Hong-Peng Qu(曲洪鹏), Guang-Zhou Hao(郝广周)
Southwestern Institute of Physics, Chengdu 610041, China

(Received 11 December 2019)

We numerically investigate the effects of ion-to-electron temperature ratio T_i/T_e and temperature gradient ratio η_i/η_e on resistive ballooning modes (RBMs) under tokamak edge plasma conditions. The results show that the growth rates of the RBMs exhibit the characteristic of a quite broad poloidal wavenumber spectrum in the cold ion limit. The growth rate spectrum becomes narrower and the peak of the spectrum shifts from the short to long wavelength side with increasing T_i/T_e and η_i/η_e. The electron temperature gradient has a very weak effect on the stability of RBMs. However, the ion-to-electron temperature ratio and the temperature gradient ratio have strong stabilizing effects on short-wavelength RBMs, while they have relatively weak effects on long-wavelength RBMs.

PACS: 28.52.Av, 52.30.Cv, 52.30.Ex DOI: 10.1088/0256-307X/37/6/062801

It has been generally recognized that tokamak plasma is a highly complex nonlinear system which involves various kinds of magnetohydrodynamic (MHD) modes and microinstabilities that dominate the plasma transport and hence the confinement.[1–3] Theories and experiments have indicated that anomalous transport in the plasma core can be largely controlled by drift-wave instabilities such as ion temperature gradient (ITG) mode,[4] trapped electron mode (TEM)[5] and electron temperature gradient (ETG) mode.[6] However, turbulence in a more collisional plasma edge is rather different due to the collisional nature, suggesting that resistive edge modes may be an important source of turbulence.[7] Thus, physical understanding of the turbulent transport still remains the most challenging problem in plasma theory, especially in plasma edge.[8]

Recent theories and simulations have suggested that the resistive ballooning mode (RBM),[9–11] which is a quite robust instability for typical edge plasma conditions, may play a significant role in driving turbulence at the plasma edge. Gyrokinetic simulations using DIII–D,[12] Tore Supra and JET L mode edge parameters[13] have indicated that the RBMs are linearly unstable and may be related to the onset of H mode.[14] Although most works have assumed "realistic" in the sense that they have taken $T_i = T_e$ and $\eta_i = \eta_e$, or $T_i = 0$ and $\eta_i = 0$, this assumption is not satisfied at the plasma edge in general, where $T_{i,e}$, and $\eta_{i,e}$ are the ion/electron temperature and ion/electron temperature gradient critical parameters, respectively. Experimental measurements usually show that T_i/T_e and η_i/η_e are larger than unity, particularly in neutral beam heated edge plasmas such as Tore Supra,[15] TEXTOR,[16] and HL-2A.[17] Therefore, ion-to-electron temperature ratio and ion-to-electron temperature gradient ratio should have considerable effects on the resistive ballooning instabilities. So far, little literature has addressed this important issue, which is the motivation of the present study.

In this work, a collisional plasma analogous to the edge region of typical L mode discharges is considered, in which the effect of trapped electrons is not expected since the bounce frequency is less than the electron-ion collision rate. The two-fluid model based on the Braginskii equations[18] describing drift resistive ballooning mode in a low-beta equilibrium for the density gradient driven RBMs are the ion continuity equation, electron continuity equation and electron parallel motion equation as follows:

$$\partial_t n_i + \nabla \cdot (n_i \boldsymbol{u}_i) = 0, \tag{1}$$

$$\partial_t n_e + \nabla \cdot (n_e \boldsymbol{u}_e) = 0, \tag{2}$$

$$0 = -\nabla_{||} p_e + en\nabla_{||}\varphi + en\partial_t A + enj_{||}/\sigma_{||}. \tag{3}$$

Here we define $n_{i,e}$, $\boldsymbol{u}_{i,e}$, p_e, E and B to be the ion/electron density, ion/electron velocity, electron pressure, electric field and magnetic field, respectively. The plasma quasi-neutrality $n_i = n_e = n$ has been assumed. The parallel current density and conductivity are $j_{||} = -enu_{e||}$ and $\sigma_{||} = \frac{2e^2 n}{m_e \nu_e}$, with $\nu_e = \frac{n_e e^4 \ln \Lambda}{3(2\pi)^{3/2} m_e^{1/2} T_e^{3/2}}$ is the electron-ion collision rate and $\ln\Lambda$ is the Coulomb logarithm. The velocities neglecting the ion parallel motion can be written as

$$\boldsymbol{u}_i = \boldsymbol{u}_E + \boldsymbol{u}_{*i} + \boldsymbol{u}_{Pi}, \tag{4}$$

$$\boldsymbol{u}_e = \boldsymbol{u}_E + \boldsymbol{u}_{*e} + u_{e||}\boldsymbol{b}, \tag{5}$$

where $\boldsymbol{u}_E = \frac{\boldsymbol{b}\times\nabla\varphi}{B}$ is the $\boldsymbol{E}\times\boldsymbol{B}$ drift velocity, $\boldsymbol{u}_{*i,e} = \frac{\boldsymbol{b}\times\nabla p_{i,e}}{en_{i,e}B}$ is the ion/electron diamagnetic drift velocity, $u_{e||}$ is the electron parallel velocity and $\boldsymbol{b}$ is the magnetic unit vector, respectively. The ion polarization

*Supported by the National Key R&D Program of China (Grant Nos. 2017YFE0300405 and 2017YFE0301200) and the National Natural Science Foundation of China (Grant Nos. 11775067, 11775069, 11875019, and 11805058).
**Corresponding author. Email: xujq@swip.ac.cn
© 2020 Chinese Physical Society and IOP Publishing Ltd

drift velocity is given by $\boldsymbol{u}_{\rm Pi} = -\frac{m_{\rm i}}{eB^2}\partial_t \nabla_\perp \varphi$. Substituting each velocity into Eqs. (1)–(3) with the linearization and Fourier transformation for all of the perturbed quantities, we can obtain the set of eigen equations as follows:

$$\omega\hat{n} + \omega k_\perp^2\rho_{\rm s}^2\hat{\varphi} = -\tau_{\rm i}\omega_{\rm De}\hat{n} + [\omega_{*\rm e} - \tau_{\rm i}\omega_{\rm De} - \tau_{\rm i}(1+\eta_{\rm i})\omega_{*\rm e}k_\theta^2\rho_{\rm s}^2]\hat{\varphi}, \quad (6)$$

$$\omega k_\perp^2\rho_{\rm s}^2\hat{\varphi} = -(1+\tau_{\rm i})\omega_{\rm De}\hat{n} + \beta_{\rm e}^{-1}k_{||}c_{\rm s}k_\perp^2\rho_{\rm s}^2\hat{A}_{||}, \quad (7)$$

$$\omega\hat{A}_{||} = k_{||}c_{\rm s}(\hat{\varphi}-\hat{n}) + \left(\omega_{*\rm e} - i\frac{m_{\rm e}\nu_{\rm e}}{2m_{\rm i}\beta_{\rm e}}k_\perp^2\rho_{\rm s}^2\right)\hat{A}_{||}, \quad (8)$$

where $\mu_0 j_{||} = -\nabla_\perp^2 A_{||}$. The notations ω, $\omega_{*\rm e} = -\frac{T_{\rm e0}\boldsymbol{k}\cdot\boldsymbol{b}\times\nabla n_{\rm e0}}{en_{\rm e0}B}$ and $\omega_{\rm De} = [2g(\theta)/g_{\rm n}]\omega_{*\rm e}$ are the eigenvalue of the mode, electron diamagnetic drift frequency and the magnetic drift frequency, respectively. The function $g(\theta) = \cos\theta + [\hat{s}\theta - \alpha\sin\theta]\sin\theta$ implies the magnetic field bending with θ being the poloidal angle. All the perturbed quantities are normalized as $\hat{n} = \tilde{n}_{\rm i}/n_{i0} = \tilde{n}_{\rm e}/n_{\rm e}$, $\hat{\varphi} = e\tilde{\varphi}/T_{\rm e}$, $\hat{A}_{||} = ec_{\rm s}\tilde{A}_{||}/T_{\rm e}$, which are the dimensionless forms of the perturbed density, electrostatic potential, and parallel component of vector potential, respectively. In addition, $\tau_{\rm i} = T_{\rm i}/T_{\rm e}$, $c_{\rm s} = \sqrt{T_{\rm e}/m_{\rm i}}$, $\rho_{\rm s} = m_{\rm i}c_{\rm s}/eB$, and $\beta_{\rm e} = \mu_0 n_{\rm e}T_{\rm e}/B^2$ are the ion-to-electron temperature ratio, the ion sound velocity, the ion sound Larmor radius and the electron dynamical beta, respectively; $g_{\rm n} = -R\nabla n_{\rm e}/n_{\rm e}$, $g_{T_{\rm i,e}} = -R\nabla T_{\rm i,e}/T_{\rm i,e}$ and $\eta_{\rm i,e} = g_{T_{\rm i,e}}/g_{\rm n}$ represent the normalized density, ion/electron temperature gradient and the ion/electron temperature gradient critical parameter, respectively. The eigenvalues are normalized by $\omega_{\rm De0} = 2k_\theta\rho_{\rm s}c_{\rm s}/R$. The high–$n$ ballooning mode formalism referred as ballooning transformation[19] is applied thus we have

$$k_\perp^2\rho_{\rm s}^2 = k_\theta^2\rho_{\rm s}^2[1+(\hat{s}\theta-\alpha\sin\theta)^2], \quad k_{||} = -\frac{i}{Rq}\frac{d}{d\theta}, \quad (9)$$

where k_θ and $k_\perp$ denote the poloidal and perpendicular wave numbers, respectively; $\alpha = 2(1+\tau_{\rm i})\beta_{\rm e}q^2[g_{\rm n} + g_{T_{\rm e}}/(1+\tau_{\rm i}) + \tau_{\rm i}g_{T_{\rm i}}/(1+\tau_{\rm i})]$ is the plasma MHD pressure gradient parameter, $\hat{s} = d\ln q/d\ln r$ is the magnetic shear, q is the safety factor, R is the major radius of a tokamak, and r is the radial coordinate. The eigenvalue and eigenvector of the set of Eqs. (6)–(8) are easily to obtain by using the generalized eigenvalue algorithm through the standard numerical method, from which the growth rate and real frequency are estimated.

We now solve the set of eigen Eqs. (6)–(8) and describe a study on the effect of $\tau_{\rm i}$ and $\eta_{\rm i}/\eta_{\rm e}$ on the linear stability of RBM under the typical L-mode edge plasma condition. The parameters corresponding to medium-sized tokamak edge parameters are assumed as follows: $R = 2.0\,{\rm m}$, $a = 0.5\,{\rm m}$, $B = 1.5\,{\rm T}$, $q = 4$ and $\hat{s} = 3$. The dependence of growth rate on $\tau_{\rm i}$ is estimated at $n_{\rm e} = 2.0\times10^{19}\,{\rm m}^{-3}$, $T_{\rm e} = 50\,{\rm eV}$ and $g_{\rm n} = R/L_{\rm n} = 20$ throughout this study unless stated otherwise. Figure 1 shows the eigenmode structure of the RBM in the ballooning space in the limits of $\tau_{\rm i} = 0$ and $\eta_{\rm i} = \eta_{\rm e} = 0$ as an example. It can be easily demonstrated that the mode structures are similar under different parameters except that the structure will exhibit a more localized feature as the RBM becomes more unstable. The structure has the characteristics of even parity, strong ballooning structure localized near $\theta = 0$, and electrostatic potential substantially larger than that of the magnetic one. Physically, RBM is essentially the resistive MHD-type mode, which has mode structure consisting of two separated regions. One is the very narrow inner resistive layer $\theta < \pi$ and the other the broad outer ideal region $\theta \geq \pi$.[20] This kind of structure typically occurs in the relatively high collisional regime such as the L-mode edge parameters.

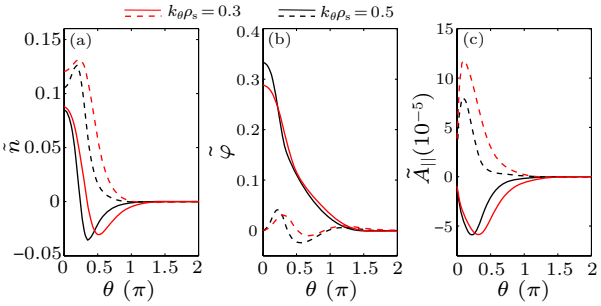

Fig. 1. Eigenmode structure of the RBM: (a) density fluctuation $\tilde{n}$, (b) electrostatic potential fluctuation $\tilde{\varphi}$, and (c) magnetic potential fluctuation $\tilde{A}_{||}$ in the ballooning space θ for $k_\theta\rho_{\rm s} = 0.3$ and $k_\theta\rho_{\rm s} = 0.5$. The solid and dashed lines represent the real and imaginary parts, respectively.

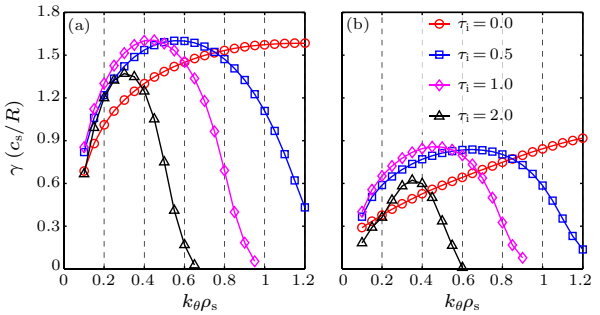

Fig. 2. Poloidal wavenumber spectrum of the growth rate for (a) $T_{\rm e} = 50\,{\rm eV}$ and (b) $T_{\rm e} = 100\,{\rm eV}$.

Figure 2(a) shows the growth rate spectrum as a function of the poloidal wavenumber for different $\tau_{\rm i}$ with $\eta_{\rm i} = \eta_{\rm e} = 0$ calculated at $T_{\rm e} = 50\,{\rm eV}$, illustrating the feature of a quite broad poloidal wavenumber spectrum in the cold ion limit $\tau_{\rm i} = 0$. This characteristic may be related to the broad band frequency spectrum of turbulent fluctuations observed in experiments. It is realized that the spectrum strongly depends on $\tau_{\rm i}$, with its peak point moving to the lower wavenumber side and becoming more narrower as $\tau_{\rm i}$ increases, indicating that a larger value of $\tau_{\rm i}$ is needed to stabilize the longer-wavelength RBMs. A strong stabilizing effect of ion temperature on the short wavelength RBMs is observed, which is enhanced with the increasing $\tau_{\rm i}$. The modes with wavelength comparable and larger

than the ion gyro-scale can be fully suppressed if the ion temperature or its gradient becomes larger than that of the electron. In addition, the long-wavelength RBMs with $k_\theta\rho_s < 0.3$ seem to be unaffected in the situation of $\tau_i \leq 2$. Similar features are observed for $T_e = 100$, as shown in Fig. 2(b). Here the growth rates are reduced due to the stabilizing effect for T_e and the peak growth rate is shifted to a smaller wavelength. The long-wavelength modes are also stabilized by the large τ_i in the high T_e situation. It should be pointed out that the growth rates estimated with relatively large wavenumber ($k_\theta\rho_s > 1$) may not be quite as accurate as the model derived previously which only considered part of the finite Larmor radius effect (FLR) on the electrostatic potential. A more accurate gyrofluid or gyrokinetic model will be constructed and discussed in future works.

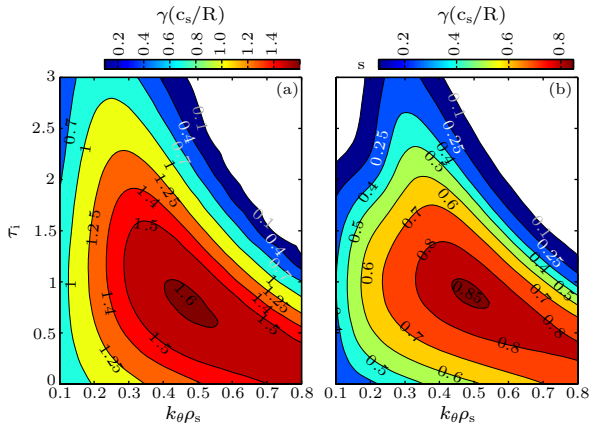

Fig. 3. The growth rate spectrum of RBMs as a function of $k_\theta\rho_s$ and τ_i for (a) $T_e = 50$ eV and (b) $T_e = 100$ eV.

Figure 3 shows the detailed linear stability property of RBMs as functions of $k_\theta\rho_s$ and τ_i with $\eta_i = \eta_e = 0$, where (a) and (b) are calculated at $T_e = 50$ eV and $T_e = 100$ eV, respectively. We observe that a clear reduction of the grow rate γ due to the ion temperature with the peak value occurring at $k_\theta\rho_s \sim 0.4$–0.6 and $\tau_i \sim 0.5$–1. It is indicated that even for the very large τ_i cases, the modes with wavenumber $k_\theta\rho_s \sim 0.1$–0.3 have considerable growth rates, which seems to be consistent with the experimental measured density fluctuations with the peak value of wavenumber spectrum at $k_\theta\rho_i \sim 0.1$–0.2.[21] The maximum of the growth rate spectrum shifts to the low wavenumber side accompanied with the stabilization of the short wavelength modes. The modes with scale $k_\theta\rho_s < 0.3$ are weakly destabilized by relatively small τ_i. However, the short wavelength RBMs are rapidly stabilized as τ_i increases, which is partially demonstrated in Fig. 3. Thus, a strong auxiliary heating method of the ion temperature such as neutral beam injection (NBI) or ion cyclotron resonance heating (ICRH) may be helpful for suppressing the high frequency turbulence in tokamak edge plasmas.

In order to investigate the dependence of the growth rate of RBMs on the ion temperature gradient, it is necessary to firstly discuss the effect of electron temperature gradient on the linear stability of the mode. It is found that the η_e has a very weak effect on RBMs, as indicated in Fig. 4(a) with $\eta_i = 0$. This is easily understood from the model equations that η_e does not enter them but has only a weak effect on the MHD parameter α. Here we have assumed $\tau_i = 1$ as it should be included if we investigate the effect of η_i, which is found to be coupled with τ_i in Eq. (6). The growth rate spectrum with different η_i is depicted in Fig. 4(b). Compared with Fig. 3, both the η_i and τ_i have stabilizing effects on large wavenumber modes, except that effect of η_i is weaker than that of τ_i.

The detailed parameter dependence of the growth rate on the temperature gradient ratio is shown in Fig. 5, where we have assumed $\eta_e = 1$ and $\tau_i = 1$. It is clearly seen, similar to that of τ_i, the η_i has stabilizing effect on short-wavelength RBMs but a weak effect on long-wavelength modes with the peak of the spectrum shifts from high wavenumber to the long-wavelength side. Compared with that of the τ_i, the effect of the temperature gradient ratio appears to be less significant, which is also partially demonstrated in Fig. 5.

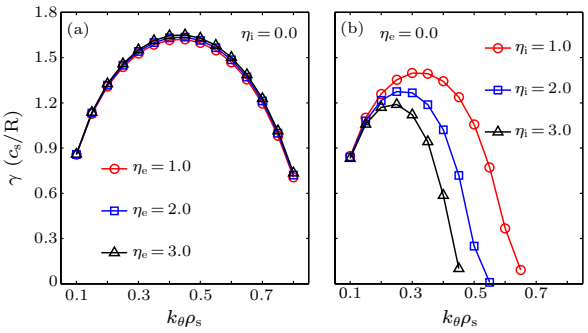

Fig. 4. Dependence of the growth rate spectrum on temperature gradient, calculated at (a) $\eta_i = 0$ and (b) η_e=0.

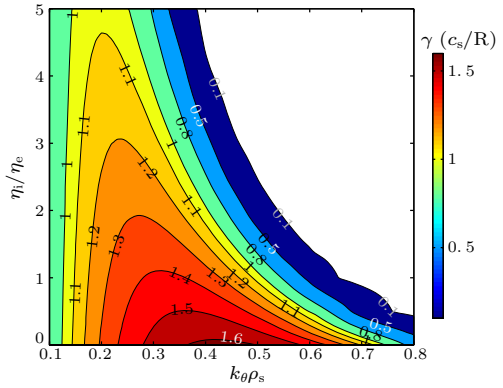

Fig. 5. The growth rate spectrum of RBMs as a function of $k_\theta\rho_s$ and η_i with $\tau_i = \eta_e = 1$.

We now check how the growth rate spectrum of the RBM changes with the ion-to-electron temperature ratio and temperature gradient ratio. Figure 6 shows the two-dimensional joint distribution of the growth rate spectrum in the parameter space of τ_i and η_i/η_e, which is estimated at $\eta_e = 1$. Here we have chosen

the wavenumber $k_\theta\rho_s = 0.3$ and $k_\theta\rho_s = 0.5$ as the spectrum peak around them in our parameter scan. For the case of $k_\theta\rho_s = 0.3$, the max growth rate occurs at $\tau_i \sim 0.8$–1.5 and relatively small $\eta_i < 0.5$, which are in the range of typical ohmic and L mode edge plasma parameters, suggesting that the density gradient driven RBMs are highly unstable under the present L mode plasma edge-like conditions, as can be seen in Fig. 6(a). The mode is strongly damped as the τ_i and η_i increase. Moreover, it is noted that the growth rate of RBMs is slighted reduced with a small τ_i even uf η_i is large enough, implying that the ion temperature itself is more efficient in stabilizing the RBMs than its gradient. Similar results have been found for the case of $k_\theta\rho_s = 0.5$, in addition to the fact that the spectrum becomes narrower and the peak moves to smaller $\tau_i \sim 0.5$–1, indicating that the ion temperature and its gradient have a stronger stabilizing effect on relatively short-wavelength RBMs than the low wavenumber one, as seen in Fig. 6(b). From this prospective, it is implied that an external heating of ions is necessary to suppress the short wavelength resistive ballooning turbulence in the edge region, which should hence have significant advantages in improving the global plasma confinement.

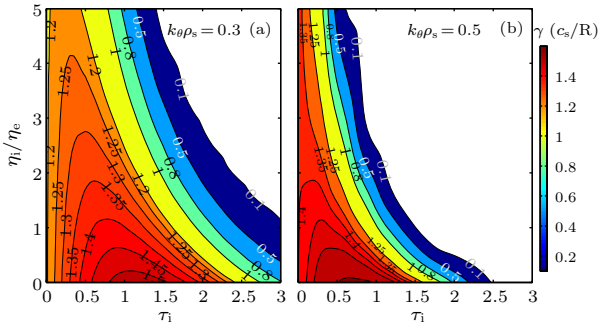

Fig. 6. Joint distribution of growth rate spectrum of RBMs as functions of τ_i and η_i/η_e for (a) $k_\theta\rho_s = 0.3$ and (b) $k_\theta\rho_s$=0.5.

In summary, we have studied the effect of ion-to-electron temperature ratio τ_i and gradient ratio η_i/η_e on the density gradient driven resistive ballooning modes. The numerical results show that the peak of the growth rate spectrum shifts from high to low wavenumber side accompanied with a stabilization of the short-wavelength modes with the increasing ratios. The value of τ_i required to stabilize the RBM is increased as the wavelength becomes longer. The modes with wavelength comparable and larger than the ion gyro-scale can be fully suppressed as long as $\tau_i > 1$. The electron temperature gradient η_e has a rather weak effect on RBMs whereas the ratio η_i/η_e has a stabilizing effect on short wavelength RBMs as well as a weak influence on the long wavelength ones. Moreover, it is implied that the effect of the ion temperature gradient is less significant than that of the ion temperature itself. These results may provide a possible explanation of the edge transport due to long-wavelength turbulence in ohmic or L mode edge plasmas and the suppression of high frequency turbulence during L–H transitions with strong neutral beam injection.

References

[1] Horton W 1999 *Rev. Mod. Phys.* **71** 735
[2] Wesson J A 1978 *Nucl. Fusion* **18** 87
[3] Tang W M 1978 *Nucl. Fusion* **18** 1089
[4] Hammett G W, Beer M A, Dorland W, Cowley S C and Smith S A 1993 *Plasma Phys. Control. Fusion* **35** 973
[5] Coppi B, Migliuolo S and Pu Y K 1990 *Phys. Fluids B* **2** 2322
[6] Dorland W, Jenko F, Kotschenreuther M and Rogers B N 2000 *Phys. Rev. Lett.* **85** 5579
[7] Myra J R, D'Ippolito D A, Xu X Q and Cohen R H 2000 *Phys. Plasmas* **7** 4622
[8] Wilson H R, Connor J W, Field A R, Fielding S J, Hastie R J, Miller R L and Taylor J B 2000 *Nucl. Fusion* **40** 713
[9] Moore R W, Dominguez R R and Chu M S 1985 *Nucl. Fusion* **25** 1575
[10] Strauss H R 1981 *Phys. Fluids* **24** 2004
[11] Bateman G and Nelson D B 1978 *Phys. Rev. Lett.* **41** 1804
[12] Cohen B I, Umansky M V, Nevins W M, Makowski M A, Boedo J A, Rudakov D L, McKee G R, Yan Z and Groebner R J 2013 *Phys. Plasmas* **20** 055906
[13] Bourdelle C, Garbet X, Singh R and Schmitz L 2012 *Plasma Phys. Control. Fusion* **54** 115003
[14] Bourdelle C, Maggi C F, Chôné L, Beyer P, Citrin J, Fedorczak N, Garbet X, Loarte A, Millitello F, Romanelli M, Sarazin Y and Contributors J E 2014 *Nucl. Fusion* **54** 022001
[15] Kočan M, Gunn J P, Pascal J Y, Bonhomme G, Fenzi C, Gauthier E and Segui J L 2008 *Plasma Phys. Control. Fusion* **50** 125009
[16] Stejner M, Salewski M, Korsholm S B, Bindslev H, Delabie E, Leipold F, Meo F, Michelsen P K, Moseev D, Nielsen S K, Bürger A and de Baar M 2013 *Plasma Phys. Control. Fusion* **55** 085002
[17] Yu D L, Wei Y L, Liu L, Dong J Q, Ida K, Itoh K, Sun A P, Cao J Y, Shi Z B, Wang Z X, Xiao Y, Yuan B S, Du H R, He X X, Chen W J, Ma Q, Itoh S I, Zhao K J, Zhou Y, Wang J, Ji X Q, Zhong W L, Li Y G, Gao J M, Deng W, Yi L, Xu Y, Yan L W, Yang Q W, Ding X T, Duan X R, Yong Liu and Team A 2016 *Nucl. Fusion* **56** 056003
[18] Braginskii S I 1965 *Rev. Plasma Phys.* **1** 205
[19] Connor J W, Hastie R J and Taylor J B 1978 *Phys. Rev. Lett.* **40** 396
[20] Drake J F and Antonsen T M 1985 *Phys. Fluids* **28** 544
[21] Liewer P C 1985 *Nucl. Fusion* **25** 543